Surfactants in Solution, Vol. 6 (K. L. Mittal & P. Bothorel, Eds.)
Plenum Press, New York, 1987, pp. 1537-1547.

A NEW METHOD FOR MEASURING FILM AND LINE TENSIONS

A. D. Nikolov, P. A. Kralchevsky and I. B. Ivanov

Laboratory of Thermodynamics and Physico-Chemical Hydrodynamics, Faculty of Chemistry
University of Sofia, 1126 Sofia, Bulgaria

A new method for measuring the film and line tensions γ and κ is described. It is applicable to a bubble (or drop) attached to a liquid surface. Perturbational equations for the lower bubble surface, the cap of the bubble (the film) and the external meniscus are derived. The radius of the contact line, r_c, and the equatorial bubble radius, R, are measured optically. The radius of curvature of the film, R_f, is determined from the experimental differential interferometric pattern (by the shearing method) and the equations of the bubble cap and the external meniscus. The film and line tensions are calculated from the measured values of r_c, R and R_f, the equations of the three surfaces and the conditions for mechanical equilibrium. The measured film and line tensions for bubbles in solutions of sodium laurylsulfate exhibit a strong dependence on the film curvature and unexpectedly large values of the (negative) line tension. The results are in qualitative agreement with the theory of Churaev, Starov and Derjaguin and the results of Torza and Mason.

INTRODUCTION

The interest in the line tension has been growing during the last decade. To a large extent it was stimulated by the role of the line tension in the occurence of a number of processes of practical importance, e.g. heterogeneous nucleation[1,2], flotation of ores[3], droplets coalescence in emulsions[4], microbial adhesion[5] etc. Line tension effects may prove important for other phenomena like membrane fusion, plasmapheresis etc. The

line tension can, in principle, be measured by studying any phenomenon that is affected by it, e.g. from the rate of heterogeneous nucleation[2]. This approach requires, however, knowledge (and/or fitting) of several parameters. Therefore, it is better to determine the line tension directly from the conditions for mechanical equilibrium of small particles at another interface.

The experimental method we used to obtain bubbles of different radii is essentially the "shrinking bubble method" of Princen and Mason[6]. A relatively large bubble at the liquid surface is allowed to decrease gradually its volume due to the escaping gas through the thin film, and its geometrical parameters are recorded optically as a function of the time. The major outcome of our study was the conclusion that both the film and line tensions of very small films depend strongly on the geometrical parameters of the system.

BASIC EQUATIONS

Our final aim is to calculate the film and line tensions γ and κ respectively from the experimentally measured values of the solution surface tension σ, the radius, r_c, of the contact line, the radius, R, of the maximum cross-section of the bubble parallel to the liquid surface, and the radius of curvature, R_f, of the film (the hat). This is done by using the force balance equations:

$$\gamma/\sigma = (\sin\phi_c + \sin\psi_c)/\sin\theta \ , \tag{1}$$

$$\kappa/\sigma = r_c\{ \cos\phi_c + \cos\psi_c - (\sin\phi_c + \sin\psi_c)\mathrm{ctg}\theta \} \ , \tag{2}$$

where θ, ϕ_c and ψ_c are the angles at which the film, bubble and external meniscus surfaces meet the plane $z=z_c$ - see Fig.1. Here we only summarize the pertinent equations, derived in ref.7, and show how ϕ_c and ψ_c can be calculated from the measured values of r_c, R and R_f.

Since the film is part of a sphere, θ is obtained directly from r_c

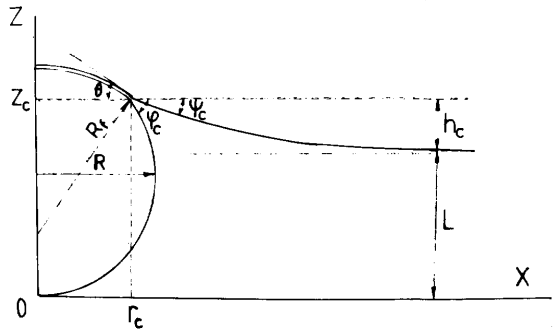

Figure 1. Scheme of a bubble of equatorial radius R, attached to a liquid surface.

and R_f :

$$\sin\theta = r_c/R_f \ . \qquad (3)$$

Equations for the shape of the surfaces of the bubble and the external meniscus were derived in ref.7 in terms of the small parameters

$$\beta = \Delta\rho\ g\ b^2 / \sigma \qquad \text{and} \qquad \varepsilon = (\Delta\rho\ g\ r_c^2 / \sigma)^{1/2} \qquad (4)$$

where b is the radius of curvature at the bottom of the bubble (at z=0), g is the acceleration due to the gravity, and $\Delta\rho$ is the density difference between the liquid and the gas phase. In our experiments ($b \approx R \leq 150$ μm and $r_c \leq 50$ μm) $\beta < 8\times10^{-3}$ and $\varepsilon < 3\times10^{-2}$. This allows one to obtain all numerical results by iterative procedures. The quantities b and β (see Equation (4)) are calculated from the measured value of R :

$$1/b = \{1 - \beta/6 + \beta^2(\ln 2 - 1/6)/6\}/R \qquad (5)$$

using as zeroth approximation $b^{(o)} = R$. With this result for β, one calculates ϕ_c as :

$$\sin\phi_c = \frac{r_c}{b} - \beta\left(\frac{1}{3}\mathrm{ctg}\frac{\phi_c}{2} - \frac{1}{6}\sin 2\phi_c - \frac{1}{2}\sin\phi_c\right)$$
$$- \beta^2\left\{\left(\frac{3}{4} + \frac{1}{2}\cos\phi_c - \frac{2}{9}\sin^2\phi_c - \frac{1}{3}\ln\sin\frac{\phi_c}{2}\right)\sin\phi_c\right.$$
$$\left. - \frac{1}{2}\left(1 + \frac{1}{9}\mathrm{ctg}^2(\phi_c/2)\right)\mathrm{ctg}(\phi_c/2)\right\} , \qquad (6)$$

using $\phi_c^{(o)} = \arcsin(r_c/b)$ as the zeroth approximation.

Since ψ_c is related to ϕ_c, we need a relationship between these quantities. It is provided by the condition for the constancy of the pressure differences between all points of two horizontal planes situated in the bulk gas and liquid phases[8]:

$$\frac{2\gamma}{R_f} - \frac{2\sigma}{b} = \Delta\rho g L. \qquad (7)$$

Since $L = z_c - h_c$, where $z_c = z(\phi_c)$, Equation (7) along with Equations (1), (3) and (4), leads to the desired relationship between ψ_c and ϕ_c:

$$\sin\psi_c = \frac{r_c}{b}\left\{1 + \frac{\beta}{2b}(z_c - h_c)\right\} - \sin\phi_c \ . \qquad (8)$$

In this equation z_c and h_c are given by[7]:

$$z_c = b\left\{1 + \cos\phi_c + \beta\left(\frac{1}{3}\sin^2\phi_c + \frac{2}{3}\ln\sin(\phi_c/2) - (1 + \cos\phi_c)/2\right)\right\} , \qquad (9)$$

$$h_c = r_c\sin\psi_c \ \ln\frac{4}{\gamma_e\sqrt{\Delta\rho g/\sigma}\ r_c(1 + \cos\psi_c)} \ , \qquad (10)$$

where $\gamma_e = 1.781\ 072\ 418\ \ldots$ is Euler's number. The zeroth approximation to be used in Equation (8) when calculating ψ_c is $h_c = 0$, i.e. $\psi_c^{(o)} = 0$.

The set of Equations (1) to (6) and (8) allows the calculation of film

and line tensions γ and κ only from the experimental values of r_c, R and R_f at a given time t without making any additional hypothesis. The only assumption that was tacitly made was that the bubble surface and the external meniscus have the same surface tension, σ.

EXPERIMENTAL PROCEDURE AND MATERIALS

The experiments were carried out with 0.05% (1.73×10^{-3} kmol/m^3) solutions of dodecyl sodium sulfate (Fisher Scientific, for high performance liquid chromatography) and two concentrations of NaCl (Merck, analytical grade) - 0.25 and 0.32 kmol/m^3. All experiments were carried out in a thermostated room at $22\pm0.5^{\circ}$C. The surface tensions of the two solutions used, with 0.25 and 0.32 kmol/m^3 NaCl, were 32.4 and 31.7 mN/m (dyn/cm) respectively. The essential part of the measurement cell (the one containing the solution) consists of a glass cylinder of diameter 1 cm and height 1.4 cm whose bottom is an optically plane-parallel glass. The bottom was fixed to the cylinder with glass powder heated at 500°C without using chemical seals. The air bubbles were blown out of a Hamilton syringe. The optical measurements were carried out with a microscope Epival Interphako (Carl Zeiss, Jena). The use of the shearing method is described in the next section. The values of r_c and R were recorded visually every time when the diameter of the respective circumference became equal to an integer number of scale divisions. At suitably chosen time intervals (100 - 200 s) the image was splitted and measurements of R_f were performed either by taking photographs or visually, by counting the number of interference rings.

A major experimental problem is that we need for the calculations the set of values r_c, R and R_f at a given moment, t, whereas some time elapses after the registration of each of these quantities. One possible way to find the required values is by least squares interpolation of the data for $r_c(t)$, R(t) and $R_f(t)$. We interpolated R(t) by the equation

$$R(t) = a_1(t_o - t)^q + a_2(t_o - t)t \ , \qquad (11)$$

where t_o, q, a_1 and a_2 are constants to be determined by the minimization of the dispersion

$$\Phi_1(a_1, a_2, t_o, q) = \sum_i \{R(t_i) - R_i\}^2 \ . \qquad (12)$$

Here R_i is the measured value of R at the moment t_i and $R(t_i)$ is calculated from Equation (11). Similar interpolation formulae were used for $r_c(t)$ and $R_f(t)$.

CALCULATION OF THE HAT (FILM) CURVATURE FROM THE INTERFERENCE PATTERN

The basic principle of the differential interferometry consists in splitting the original image into two images. The light beams coming from the two images interfere, thus creating a rather complicated interference pattern. An example is shown in Fig.2, where the shearing distance d = = 12.08 μm. The upper part of Fig.3 is a sketch of the cross section (in the plane xOz) of the two images of the reflecting surfaces splitted at a distance d along the x-axis. The plane xOy coincides with the contact line (of radius r_c). The lower part of the figure is a sketch of the resulting interference pattern (cf. Fig.2). One clearly discerns three regions corresponding to the interference of light reflected by the two images of the respective surfaces: (i) meniscus-meniscus (moustaches), (ii) meniscus-hat (rings) and (iii) hat-hat (streaks). In fact, all fringes are loci of points for which the distance between the reflecting surfaces satisfies the requirement

$$|z_\ell(x, y) - z_r(x, y)| = \ell_n = n\frac{\lambda}{4}; \quad n = 0, 1, 2, \ldots, \tag{13}$$

where subscripts "ℓ" and "r" denote left and right hand side images, λ is the light wavelength, and n is the order of interference. The equation of the hat is

$$z_{\ell,r} = \sqrt{R_f^2 - (x \pm d/2)^2 - y^2} - z_o, \tag{14}$$

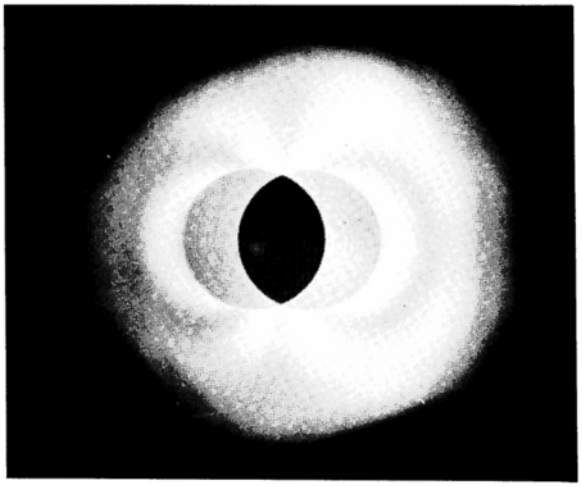

Figure 2. Differential interference pattern in light reflected from a bubble, attached to a deformed air/liquid surface (r_c = 45.4 μm, objective 25×).

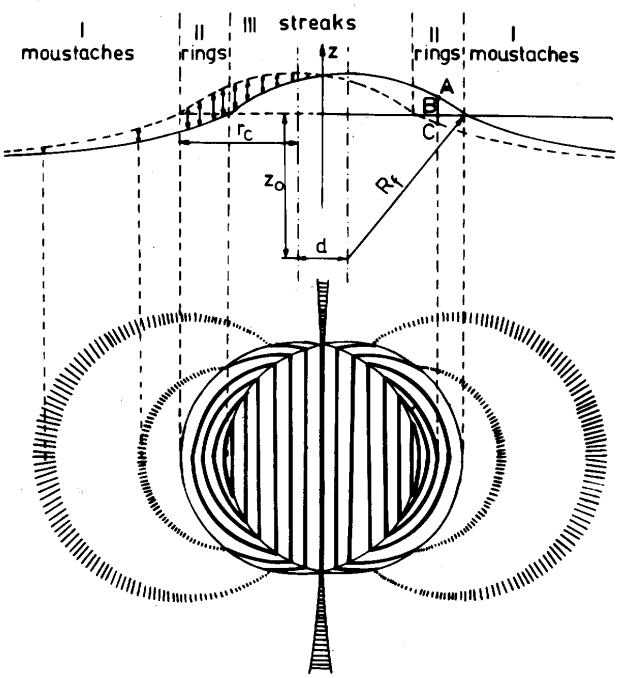

Figure 3. A sketch of the cross section of the reflecting surfaces, shifted at a distance d (upper part) and of the resulting interference pattern (lower part).

where the upper sign refers to the left hand side image, and the lower sign to the right hand side; $z_o = (R_f^2 - r_c^2)^{1/2}$ is the coordinate of the center. Thus, for region III, Equations (13) and (14) lead to

$$x^2/a_n^2 + y^2/b_n^2 = 1 \qquad (15)$$

with

$$a_n = b_n/\varepsilon_n \ , \quad b_n = (R_f^2 - \varepsilon_n^2 \ell_n^2/4)^{1/2} \ , \quad \varepsilon_n = (1 + d^2/\ell_n^2)^{1/2} \ . \qquad (16)$$

Therefore, the streaks are parts of ellipses and the reason why they look like straight lines is the high eccentricity $(1 - 1/\varepsilon_n^2)^{1/2} \approx 1$. Equation (16) allows the calculation of the hat curvature: $R_f = \varepsilon_n (a_n^2 + \ell_n^2/4)^{1/2}$ (ℓ_n, a_n and d are known from the experiment).

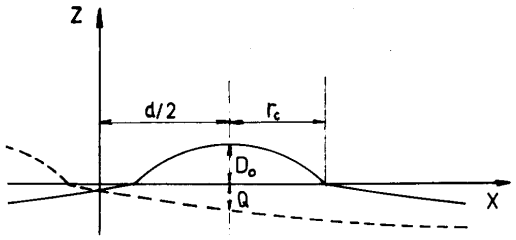

Figure 4. A scheme of the reflecting surfaces in the case of complete splitting (shearing distance $d > 2r_c$).

The visual determination of R_f was performed with complete splitting i.e. with $r_c < d/2$ (d was increased to 24.16 μm in this case in order to avoid a gap between photographic and visual measurements). The essence of the method is to record r_c at the moment when the top ring shrinks to a point. From Fig.4 it follows that at this moment $D_o + Q(d) = \ell_n$, where $Q(d) \equiv Q(x=d)$ is calculated from[7]

$$Q(x) = r_c\{ \text{arc cosh}(\frac{x}{r_c \sin\psi_c}) - \text{arc cosh}(\frac{1}{\sin\psi_c}) \}\sin\psi_c \ .$$

Then $R_f = (r_c^2 + D_o^2)/2D_o$.

RESULTS AND DISCUSSION

We have processed in full details only 4 experiments - two for the solution with 0.25 kmol/m³ NaCl (runs 1a and 1b) and two for 0.32 kmol/m³ NaCl (runs 2a and 2b). The results are presented in Figs. 5 and 6.

As explained above, when calculating γ and κ we used the data for r_c, R and R_f (at the same moment t), obtained from the interpolation curves $r_c(t)$, R(t) and $R_f(t)$ - see e.g. Equation (11). The error bars in Figures 5 and 6 denote the standard deviations of $\gamma/2\sigma$ and κ calculated by using the standard deviations of the measured radii r_c, R and R_f with respect to the interpolation curves. The points in the Figures (calculated from the smooth curves) correspond to the moments, at which R_f has been measured, and represent the most probable values of $\gamma/2\sigma$ and κ at those moments.

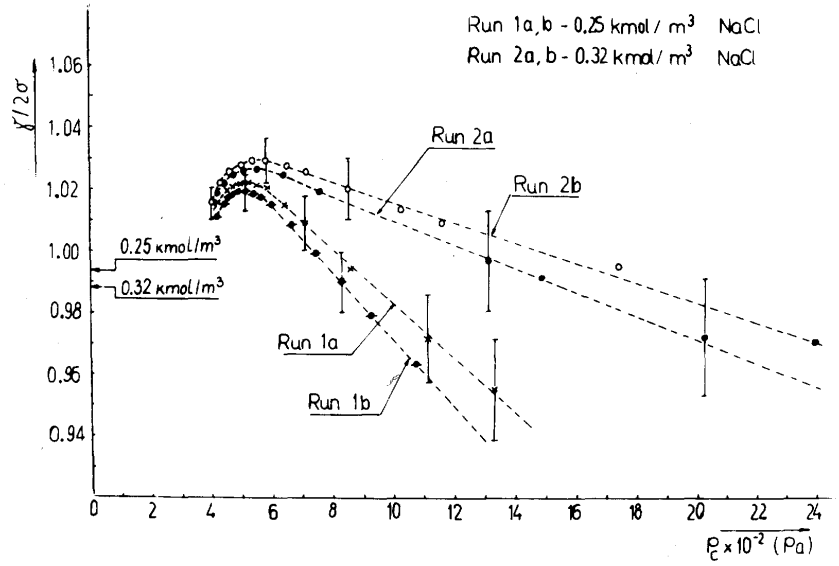

Figure 5. Dimensionless film tension $\gamma/2\sigma$ vs capillary pressure $P_c = 2\gamma/R_f$.

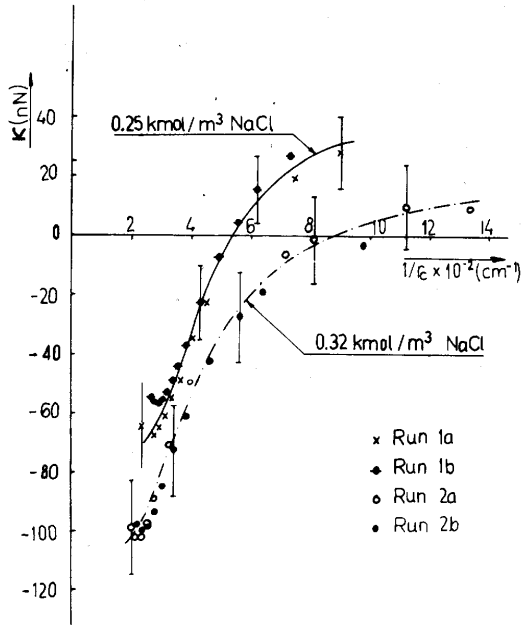

Figure 6. Line tension, κ, vs reciprocal radius r_c^{-1} of the contact line.

The most striking features in the behavior of $\gamma/2\sigma$ vs P_c are the large variations of γ (the respective values $\gamma_\infty/2\sigma$ for planar films, i.e. for $R_f \to \infty$, taken from Ref.9, are shown on the ordinate axis of Fig.5 by arrows) and the fact that at some capillary pressures γ is larger than 2σ, and this has not been observed with planar films.

Quite unexpected are the data for κ (Fig.6) - besides the large values of κ and the variation of κ with r_c, we must point out the change of sign of κ for both solutions of NaCl and to the smaller absolute values of κ for smaller bubbles i.e. for larger r_c^{-1}. There is a tendency of κ to level off for large bubbles ($r_c^{-1} \to 0$), which is more pronounced on the plot κ/σ vs R_f - Fig.7.

All these findings reveal that (unlike the surface tension and similarly to the disjoining pressure) γ and κ are strong functions of the geometrical parameters of the system. This is a new and unexpected result for γ. For the line tension this was predicted on theoretical grounds by many authors[10,11,12,13,14] but was not observed so far experimentally.

There have been only a few attempts for experimental determination of the line tension for fluid systems with configuration similar to ours. The authors of Refs. 15 and 16 have studied the same system as us (bubbles formed from solutions of sodium dodocylsulfate) but their values for κ are different from ours; for example they obtained $\kappa = 0.85$ nN for 0.32 kmol/m³. The reason for the discrepancy between our and their results lies probably in the fact that they used incomplete experimental information (they did not measure the angle θ) and to make up for this deficiency they erroneously

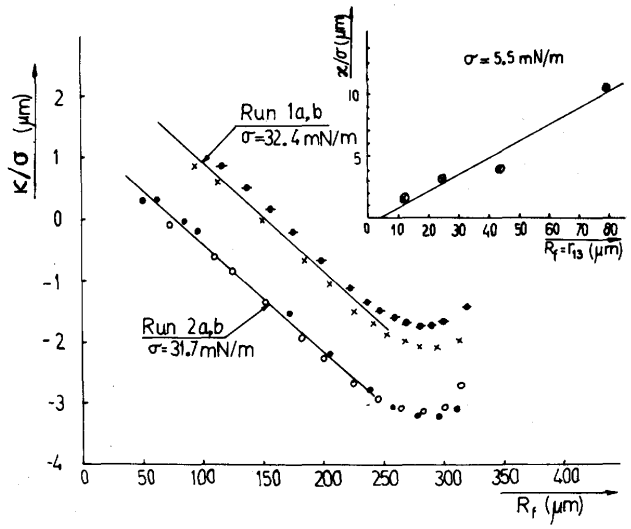

Figure 7. Dependence of κ/σ on R_f - the points correspond to runs: 1a (×), 1b (●), 2a (o), and 2b (•). The inset shows the same plot for the data of Torza and Mason[4] for doublets of emulsion droplets.

assumed that γ and κ remain constant for all bubble radii.

Navascues and Mederos[2] have determined κ from the nucleation rate of water drops on mercury. They found κ varying from -0.290 to -0.393 nN for critical radii changing from 20.7 to 25.2 nm. These low values of κ should not be surprising in view of the small size of the nuclei.

The only mesurements with particle size close to ours were carried out by Torza and Mason[4], who determined κ from the equilibrium configurations of five doublets of emulsion droplets. They obtained five different values for κ (of the order of 10 nN) and attributed these differences to scattering caused by impurities in their system. In fact, a closer inspection of their data reveals that the variation in κ may well be due to geometrical factors. Indeed, their radius of curvature r_{13} of the interface between two droplets corresponds to R_f in our experiments, and if one plots their data for κ vs R_f one obtains, as with our data, a quite good linear dependence - see inset in Fig.7.

Churaev et al.[12,13] have performed model calculations of κ for a system to some extend geometrically similar to ours: a sessile spherical drop in equilibrium with a planar thin film. They adopted the simplified disjoining pressure isoterm shown in the inset in Fig.8. If one assumes $P_c << |\Pi_2|$ and expands their equation for κ/r_c in series in terms of $\Pi_2/a\sigma$ (where $a = (\Pi_1 - \Pi_2)/t_1$), one obtains

$$\kappa/r_c \simeq (t_1 + 3\Pi_2^3/2a^2\sigma)P_c - 3\Pi_2^4/8a^2\sigma \ .$$

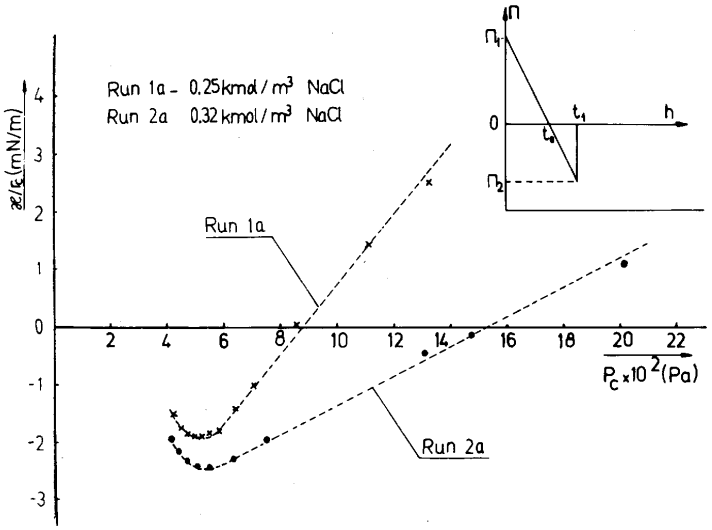

Figure 8. Plot of κ/r_c vs capillary pressure P_c.

Therefore, there should be a range of capillary pressures where κ/r_c is a linear function of P_c. Indeed, our data for κ/r_c plotted in Fig.8 as a function of P_c exhibit large linear portions. Hence, our results are in qualitative agreement with the theory of Churaev, Starov and Derjaguin. Unfortunately no quantitative comparison of the theory and the experiment is possible, because there are three unknown parameters: t_1, Π_2 and a.

For the time being we are unable to give a rigorous explanation of the effects observed by us. Yet, whatever the origin of these effects might be, we believe we have firmly established that the attachment of small bubbles to a liquid surface gives rise to unexpectedly large line tensions accompanied by corresponding variations of the film tension. Both effects are pronounced functions of the bubble and film radii. These results indicate that the conditions for equilibrium of a fluid particle at another interface are much more complicated than it was believed until now.

REFERENCES

1. R. D. Gretz, Surface Sci., 5, 239 (1966).
2. G. Navascues and L. Mederos, Surface Technol., 17, 79 (1982).
3. A. Scheludko, B. V. Toshev and D. T. Boyadjiev, J. Chem. Soc. Faraday I, 72, 2815 (1976).
4. S. Torza and S. G. Mason, Kolloid-Z. u. Z. Polym., 246, 593 (1971).
5. B. A. Pethica, in "Microbial Adhesion to Surfaces", R. C. W. Berkeley, Editor, p.19, Ellis Horwood, Chichester, U.K., 1980.

6. H. M. Princen and S. G. Mason, J. Colloid Sci., 20, 353 (1965).
7. P. A. Kralchevsky, I. B. Ivanov and A. D. Nikolov, J. Colloid Interface Sci. (in press).
8. H. M. Princen, J. Colloid Sci., 18, 178 (1963).
9. J. A. de Feijter, Thesis, Univ. Utrecht, 1973; see also J. A. de Feijter and A. Vrij, J. Colloid Interface Sci., 64, 269 (1978).
10. A. I. Rusanov, Kolloidn. Zh., 39, 704 (1977).
11. I. B. Ivanov, B. V. Toshev and B. P. Radoev, in "Wetting, Spreading and Adhesion", J. F. Padday, Editor, p.37, Academic Press, London, 1978.
12. V. M. Starov and N. V. Churaev, Kolloidn. Zh., 42, 703 (1980).
13. N. V. Churaev, V. M. Starov and B. V. Derjaguin, J. Colloid Interface Sci., 89, 16 (1982).
14. G. Navascues and P. Tarazona, Chem. Phys. Letters, 82, 586 (1981).
15. D. Platikanov, M. Nedyalkov and V. Nasteva, J. Colloid Interface Sci., 75, 620 (1980).
16. A. Scheludko, B. V. Toshev and D. Platicanov, in "The Modern Theory of Capillarity", F. C. Goodrich and A. I. Rusanov, Editors, Akademie Verlag, Berlin, 1981.